

# DNA-Encoded Immunoassay in Picoliter Drops: A Minimal Cell-Free Approach

Barbara Jacková, Guillaume Mottet,\* Sergii Rudiuk, Mathieu Morel,\* and Damien Baigl\*

Immunoassays have emerged as indispensable bioanalytical tools but necessitate long preliminary steps for the selection, production, and purification of the antibody(ies) to be used. Here is explored the paradigm shift of creating a rapid and purification-free assay in picoliter drops where the antibody is expressed from coding DNA and its binding to antigens concomitantly characterized in situ. Efficient synthesis in bulk of various functional variable domains of heavy-chain only antibodies (VHH) using reconstituted cell-free expression media, including an anti-green fluorescent protein VHH, is shown first. A microfluidic device is then used to generate monodisperse drops (30 pL) containing all the assay components, including a capture scaffold, onto which the accumulation of VHH:antigen produces a specific fluorescent signal. This allows to assess, in parallel or sequentially at high throughput (500 Hz), the VHH-antigen binding and its specificity in less than 3 h, directly from a VHH-coding DNA, for multiple VHH sequences, various antigens and down to DNA concentrations as low as 12 plasmids per drop. It is anticipated that the ultraminiaturized format, robustness, and programmability of this novel cell-free immunoassay concept will constitute valuable assets in fields as diverse as antibody discovery, point-of-care diagnostics, synthetic biology, and/or bioanalytical assays.

analyte detection to medical diagnosis,<sup>[2]</sup> their development remains time-consuming, costly, and requires dedicated human and instrumental resources. Moreover, antibody discovery has been historically strongly relying on animal immunization, rising ethical issues and increasing concerns about the necessity of animal use in such a context. For the purpose of bypassing the use of animals or animal-derived products, alternative in vitro display technologies have emerged.<sup>[3–6]</sup> The common requirements of all of these techniques are not only the efforts for the production of the antibodies but also the necessity to purify them and further characterize their affinity and selectivity for desired targets.<sup>[7]</sup> Developing an in vitro immunoassay capable of both animal-free antibody production and concomitant affinity characterization in a cost-effective fashion appears as a particularly timely challenge. To this end, one can consider using a minimal synthetic approach avoiding the use of living cells and organisms and offering both rapid antibody


## 1. Introduction

Immunoassays are ubiquitous bioanalytical techniques, in which the presence of a target molecule is detected or quantified using antibody–antigen binding interaction.<sup>[1]</sup> Despite tremendous importance in both fundamental research and real-world applications ranging from antibody discovery and

synthesis/characterization and a high degree of tunability. In particular, cell-free gene expression systems, in which a protein can be synthesized from coding DNA in a few hours, have been successfully exploited to synthesize functional proteins within a wide range of systems and applications.<sup>[8,9]</sup> Besides their versatility and commercial availability, they are advantageously compatible with cytotoxic protein synthesis, artificial amino acid incorporations,<sup>[10,11]</sup> and new methods of extrinsic expression regulation such as dynamic photocontrol.<sup>[12]</sup> By simply using DNA coding for the desired sequence, many protein types have already been synthesized including enzymes,<sup>[13–15]</sup> membrane proteins,<sup>[16–19]</sup> or large protein assemblies.<sup>[20–24]</sup> In the vast majority of current immunoassays, immunoglobulins (Igs) are used as antibodies. However, due to their large size and complex higher order structure, Ig cell-free synthesis requires substantial efforts to optimize both antibody-coding DNA sequence and the composition of cell-free expression medium.<sup>[25–27]</sup> In recent years, the variable domains of the heavy chain of heavy-chain only antibodies (VHH)<sup>[28]</sup> have emerged as interesting alternatives to Igs. Engineered from naturally occurring antibodies found in camelids, VHH is a small-sized ( $\approx 13$  kDa), stable, single-unit, and easily-foldable protein, originally used as tools for intracellular protein tracking<sup>[29]</sup> or reagents for high-affinity protein purification.<sup>[30]</sup> They nowadays represent a

B. Jacková, S. Rudiuk, M. Morel, D. Baigl  
PASTEUR  
Department of Chemistry  
École Normale Supérieure  
PSL University  
Sorbonne Université  
CNRS  
Paris 75005, France  
E-mail: mathieu.morel@ens.psl.eu; damien.baigl@ens.psl.eu

B. Jacková, G. Mottet  
Large Molecules Research Platform  
Sanofi  
Vitry-sur-Seine 94400, France  
E-mail: guillaume.mottet@sanofi.com

 The ORCID identification number(s) for the author(s) of this article can be found under <https://doi.org/10.1002/adbi.202200266>.

DOI: 10.1002/adbi.202200266

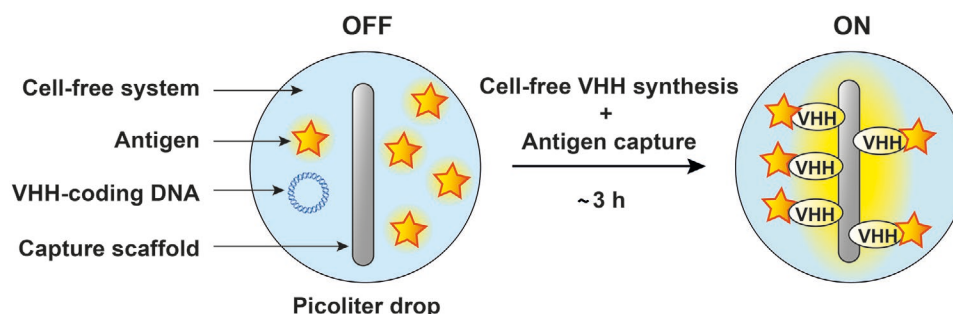


**Figure 1.** Cell-free DNA-encoded immunoassay in picoliter drops allows rapid assessment of antibody-antigen binding with minimal components, programmability, and DNA instead of the purified antibody as starting material. The concept is based on water-in-oil drops of micrometric size containing cell-free expression mix, fluorescent antigen, VHH-coding DNA, and a capture scaffold capable to attach the synthesized antibody (VHH). The resulting emulsion is incubated at 37 °C for 3 h during which the VHH is cell-free synthesized, is tethered onto the capture scaffold, and binds the antigen in case of sufficient antibody-antigen affinity. This binding alters the distribution of antigen within the drop, from unbound antigen producing a homogeneous fluorescent signal (OFF) to antigen accumulated on the capture scaffold, resulting in a local increase in fluorescence intensity (ON).

highly promising alternative to conventional therapeutic antibodies.<sup>[31,32]</sup> We thus sought after the development of a novel minimal and cell-free immunoassay principle where functional VHH would be synthesized and its affinity characterized in a single step, with reduced amounts of time and components. To meet such needs, microfluidics and lab-on-chip technologies have the required capability to dramatically decrease the volume and time of reactions while being biocompatible, versatile, and cost-effective.<sup>[33]</sup> There have been many efforts in the past decade to develop robust microfluidic approaches to implement antibody bioassays in highly miniaturized formats.<sup>[34–36]</sup> Drop microfluidics, which consists in handling, analyzing, and sorting chemical and/or biological components in nano to picoliter monodisperse drops in a high-throughput fashion, has been identified as one of the most efficient methods to reach this objective.<sup>[37–39]</sup> For instance, the development of a microfluidic platform for compartmentalization, analysis, and subsequent sorting of individual cells<sup>[40]</sup> made it possible to conduct studies on immune cells' antibody secretome that was unexplored by conventional flow cytometry. This breakthrough enabled not only a better understanding of antibody secretion dynamics<sup>[41]</sup> but also the characterization of antibody binding properties,<sup>[41,42]</sup> both of which have facilitated the discovery of antibodies with desired functionality. These achievements had in common to be based on single-cell encapsulation in drops, with a particular focus on optimizing the methodology to increase the throughput and sorting capability of the developed microfluidic devices. Handling living cells was also accompanied by intrinsic constraints to maintain cells alive, such as limited time of experiments, mild conditions, and the use of biocompatible reagents. To further accelerate, diversify, and simplify the capability of microfluidic antibody bioassays, our strategy is thus to substitute the confined secreting cell with minimal and well-defined expression machinery producing a VHH of interest from its coding DNA. Cell-free expression was already successfully achieved in miniaturized systems involving, for instance, fluorescent proteins,<sup>[43–45]</sup> enzymes,<sup>[46–49]</sup> and transcriptional regulators,<sup>[50]</sup> but, to our knowledge, has never involved the production nor characterization of functional antibodies. Conversely, the few notable examples of cell-free VHH synthesis were always achieved in a bulk format and

associated with other methods such as mRNA, ribosome, or phage displays.<sup>[51–53]</sup> Here, we propose not only to express functional VHH in microfluidic drops by cell-free expression from its coding DNA for the first time, but also to concomitantly, and in the same picoliter drops, assess the capability of the synthesized antibody to selectively capture its target antigen. We first synthesized in bulk a VHH with a high affinity toward green fluorescent protein (GFP) using a reconstituted cell-free expression system and characterized both the synthesis yield and the functionality of the synthesized VHH and other mutants. By co-encapsulating coding DNA, expression machinery, a capture scaffold, and enhanced green fluorescent protein (EGFP) antigen in microfluidic-generated picoliter drops, we assessed the antibody-antigen interaction along the course of expression inside individual drops. Finally, using a laser detection system, we determined, at a high frequency and in a large number of individual drops, the performance of this purely synthetic immunoassay in terms of a minimum number of DNA copies per drop, antigen detection limit, and capture selectivity.

## 2. Results and Discussion

### 2.1. Concept

**Figure 1** depicts the central concept of our approach. It consists in encapsulating in the same picoliter compartment, the minimal components necessary to both synthesize a desired VHH and characterize in situ its binding affinity for a target antigen. Water-in-oil drops are used to encapsulate a small number of DNA coding for the VHH, a cell-free expression medium to synthesize the VHH from DNA and specific and/or dummy antigen(s). To detect the VHH-antigen binding, the strategy consists in implementing a capture scaffold onto which VHH are tethered upon their cell-free synthesis. As a result, target antigens, initially homogeneously distributed inside the drop, accumulate on the VHH-decorated capture scaffold, resulting, in the case of labeled VHH and/or antigens in a signal accumulation from the antibodies and/or its bound antigens. This concept combines several advantages. No cell is involved, avoiding all steps of cell maintenance, and expanding the range

of conditions that can be explored. All components in the drops are supplied in a known and prescribed concentration, offering reliability and robustness. The duration of the whole assay, starting from the DNA encapsulation to the detection of the antigen-binding, is mainly determined by the cell-free expression reaction rate and is thus of the order of a few hours only. Finally, using VHH-coding DNA as starting material enables easy applicability to virtually any kind of VHH sequence while the micrometric drop format offers immediate compatibility with microfluidic handlings such as high-throughput drop production, testing, and sorting. To demonstrate this concept, we focused on a few important key steps: picoliter drop production and encapsulation of the minimal assay, in situ VHH synthesis and concomitant antigen-binding analysis, and high-frequency analysis in a large number of flowing drops. As a model antigen, we mainly used EGFP, a commonly used fluorescent target. We associated it with an anti-GFP VHH, referred here to as NanoGFP,<sup>[54]</sup> which was encoded in the encapsulated DNA. For the cell-free VHH synthesis, we focused on a reconstituted protein synthesis using recombinant elements (PURE) expression system,<sup>[55]</sup> a minimal set of recombinant components purified from *Escherichia coli*, for their well-known composition, fast protein synthesis, and commercial availability.

## 2.2. Bulk Characterization of Cell-Free Expressed VHHs

Prior to drop encapsulation, we characterized the amount of NanoGFP that could be synthesized by PURExpress in bulk and further tested its antigen recognition capability. To this end, we designed a plasmid containing the necessary elements for transcription and translation in the PURE system (T7 promoter, ribosome binding site [RBS], and T7 terminator) around the gene coding for VHH and hemagglutinin (HA) tag separated by a linker region (Figure 2A). For the VHH, we used a sequence previously optimized for expression in *E. coli*.<sup>[54]</sup> The HA tag, designed for tethering the synthesized protein onto the signal amplification scaffold, was positioned in the C-terminus to minimize any possible effect on the antigen binding at the VHH paratope region.<sup>[56]</sup> This fusion increased the protein molecular weight by 2 kDa only, leading to an overall size of 16.4 kDa. The resulting plasmid was incorporated into a conventional PURExpress mix and incubated at 37 °C for 3 h in a tube. Capillary western blot analysis of the product revealed a sharp single band, showing that the synthesized NanoGFP was properly produced and as full-length monomers only (Figure 2B). Its position was slightly above that obtained with a commercially available anti-GFP VHH of 13.9 kDa, in agreement with its expected size. Enzyme-linked immunosorbent assay (ELISA) titration revealed a yield of  $15.3 \pm 2 \mu\text{g mL}^{-1}$  of synthesized NanoGFP (Figure S1, Supporting Information). Replacing PURExpress with PUREflex, another PURE cell-free expression medium, resulted in successful yet lower-yield NanoGFP synthesis. Furthermore, adding supplements, such as disulfide bond enhancers or chaperones, did not improve the yield (Figure S1, Supporting Information), showing the interest in working with small-sized and simply structured proteins such as VHH. We next confirmed the binding activity

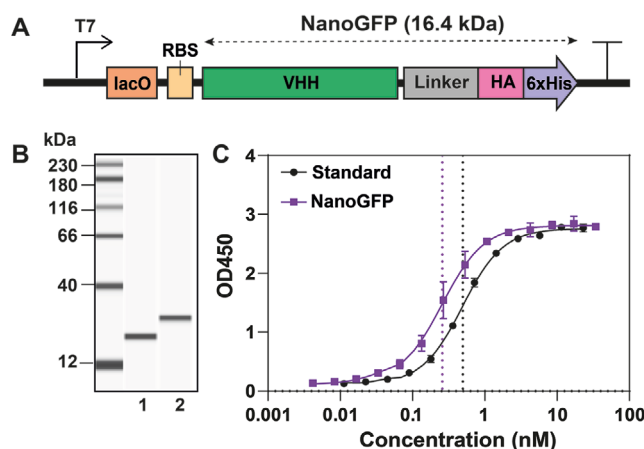


**Figure 2.** Characterization of anti-GFP VHH, called NanoGFP, expressed by PURExpress in bulk format. A) Schematic representation of the DNA template used for NanoGFP cell-free expression. The template contains T7 promoter, lac operator (lacO), and ribosome binding site (RBS) located upstream of the gene coding for NanoGFP (16.4 kDa), composed of VHH-coding gene separated by a linker from HA epitope tag and 6xHistidine tag, followed by a T7 terminator. B) Capillary western blot analysis of commercially available anti-GFP VHH (lane 1) and cell-free expressed NanoGFP (lane 2). C) Dose-response curves of commercially available anti-GFP VHH (Standard) and cell-free expressed NanoGFP. The curves were obtained by indirect ELISA, using EGFP antigen for VHH capture and an anti-VHH peroxidase-conjugated IgG for detection. The dotted lines indicate the apparent dissociation constant, for the standard:  $K_D^{app} = 0.49 \pm 0.03 \text{ nM}$  and for the NanoGFP:  $K_D^{app} = 0.26 \pm 0.03 \text{ nM}$ . NanoGFP was expressed at  $[\text{DNA}] = 4 \text{ ng } \mu\text{L}^{-1}$ , 37 °C, 3 h. Data are shown as mean  $\pm$  SD (standard deviation) on triplicated samples.

of the cell-free produced VHH. To this end, we follow the binding of EGFP as a function of NanoGFP concentration to establish the dose-response curve (Figure 2C). The method was validated with commercially available VHH (unknown complementarity determining region [CDR] sequences) leading to an apparent dissociation constant  $K_D^{app} = 0.49 \pm 0.03 \text{ nM}$ . Interestingly, the cell-free expressed NanoGFP led to a similar value  $K_D^{app} = 0.26 \pm 0.03 \text{ nM}$ , which was also in the same range as what was reported with the same VHH produced in bacteria.<sup>[29,57]</sup> All these results show that cell-free synthesis in the PURExpress system produced functional NanoGFP at conventional yield and expected binding affinity. We next exploited the DNA-encoding approach of our strategy and applied it to explore the cell-free synthesis of other VHH sequences. We started with several anti-GFP variants known for their different binding affinities and showing significant sequence diversity, especially in the CDR3 region (Figure S2, Supporting Information). Interestingly, all synthesized VHH using PURExpress also displayed a single and well-defined band in Western analysis and with expression yields ranging from  $2.6 \pm 0.1$  to  $60.7 \pm 10 \mu\text{g mL}^{-1}$ , while expression in PUREflex led to similar results yet at lower yields (Figure S3, Supporting Information). Dose-response analysis in the accessible concentration range showed functional binding activity of the synthesized mutants (Figure S4, Supporting Information). Using a cell-free expression medium from *E. coli* purified components was thus found to be a valuable strategy to synthesize significant amounts of functional anti-GFP VHH in bulk, in one step and in a few



hours only, while allowing to explore various VHH sequences by simply modifying its encoding DNA.

### 2.3. Drop Microfluidic Immunoassay

Experiments described before involved reaction volumes of about 25  $\mu\text{L}$  and a large number of DNA copies per reaction ( $10^{10}$ ). To establish a DNA-encoded immunoassay in  $10^6$ -time smaller volumes (Figure 1), we had to devise a method to confine a small number of VHH-coding DNA molecules in highly miniaturized containers and implement a method allowing to detect in situ the functionality of the synthesized VHH. The strategy was to use a microfluidic device to produce picoliter drops co-encapsulating VHH-coding DNA, the cell-free expression medium, the EGFP antigen and a capture scaffold allowing to analyze the binding of the antigen to the VHH synthesized in situ (Figure 3). This binding was assessed using a

capture nanoparticle made of a streptavidin-coated superparamagnetic bead previously functionalized with a biotinylated IgG specific to the HA tag in the C-terminus of the target synthesized VHH (Figure 3A, left). The capture nanoparticles were assembled together with the VHH-coding DNA and the EGFP antigen. This mix and PURExpress expression medium were injected at 4  $^{\circ}\text{C}$  as the two aqueous phases co-flowing at equal flow rates in a microfluidic device. Drops were generated at a flow-focusing junction with a fluorinated oil supplemented with fluorinated surfactant to ensure the non-coalescence of the produced drops<sup>[58]</sup> (Figure 3A, middle). Downstream-located serpentine ensured rapid and efficient mixing of drop components. The advantage of using capture particles of nanometric dimensions ( $\approx 300$  nm in diameter) was to enable working at a concentration high enough ( $\approx 2000$  particles per drop) to avoid heterogeneous distribution (Poisson partitioning) while offering a large surface area for binding. Our device typically produced  $2.5 \times 10^6$  drops of  $30 \pm 3$  pL of narrow polydispersity

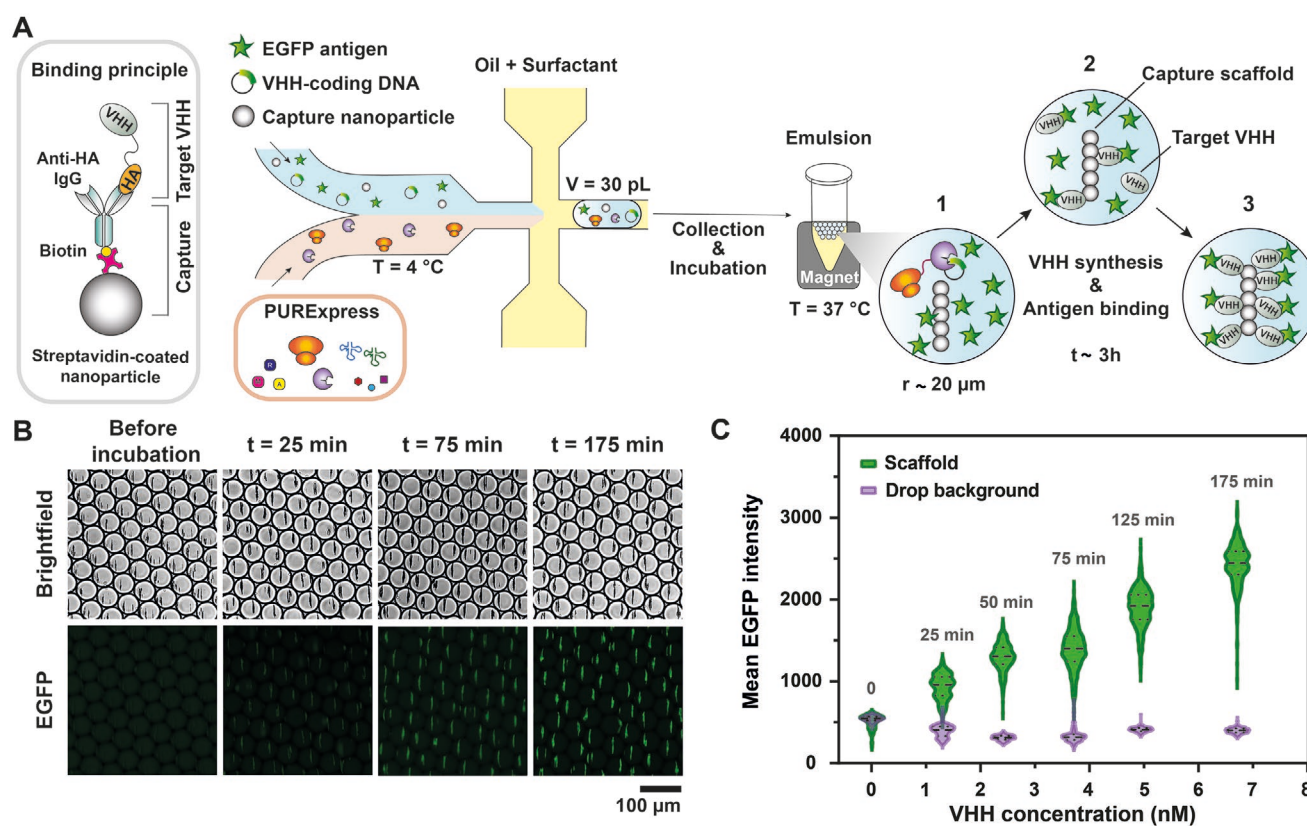


**Figure 3.** DNA-encoded immunoassay produced by microfluidics and performed with DNA coding for NanoGFP, allows for real-time in situ observation of VHH-EGFP binding thanks to the accumulation of the complex on the capture scaffold. A) Microfluidic workflow for immunoassay preparation and the mechanism of formation of fluorescent readout. Streptavidin-coated magnetic nanoparticles (300 nm in diameter) were functionalized with biotin-conjugated anti-HA IgG to allow the capture of target VHH and suspended in a solution containing VHH-coding DNA ( $\lambda = 300$  plasmids per drop) and EGFP (40 nM). The mix was injected in a droplet generator with a flow-focusing geometry, in a co-flow with PURExpress ( $400 \mu\text{L h}^{-1}$ ) and emulsified by fluorinated oil with 2% fluorosurfactant ( $1400 \mu\text{L h}^{-1}$ ), resulting in monodisperse drops of  $\approx 30$  pL. The collected emulsion was incubated at 37  $^{\circ}\text{C}$  under a magnetic field to align the magnetic nanoparticles and during 3 h the VHH was progressively synthesized (1) and tethered on the capture scaffold together with its bound EGFP (2), which produced a bright and localized fluorescence signal (3). B) VHH expression and antigen binding followed by fluorescence microscopy. After encapsulation, the emulsion was injected into a glass microfluidic chamber and imaged before and during incubation at 37  $^{\circ}\text{C}$ . C) Violin plot of the mean EGFP intensity distribution measured on the scaffold and in the drop background as a function of synthesized VHH concentration measured by sandwich ELISA on a broken emulsion. The time of incubation is indicated above each distribution. The mean EGFP intensity of  $n = 300$  droplets was assessed by particle analysis on background-subtracted images (dashed line: median, dotted lines: lower and upper quartiles). The experiment was replicated twice, showing similar results.

in 10 min. The resulting emulsion was collected and immediately incubated at 37 °C under the application of a magnetic field resulting in the formation of a bar of aligned nanoparticles<sup>[41]</sup> forming a capture scaffold in each drop (Figure 3A, right). Microscopic observation on a large number of individual drops in parallel revealed that the EGFP signal was increasing at the position of the assembled capture particles while vanishing in the background (Figure 3B and Figure S5, Supporting Information). The characteristic diffusion time for a NanoGFP:EGFP complex of 44.4 kDa was estimated to be 4.5 s (Text S1, Supporting Information) using the drop diameter as a characteristic size, allowing us to follow, with a good temporal resolution, the capture of antigen along the course of VHH expression (Figure S6A, Supporting Information), which is known to be sustained for about 3 h in bulk (Figure S7, Supporting Information). The same experiment performed without DNA resulted in no signal evolution (Figure S6B, Supporting Information), demonstrating that the increase of EGFP fluorescence in the presence of the coding DNA was resulting from the accumulation of synthesized VHH binding the antigen. To our knowledge, this constitutes the first in situ observation of antibody–antigen binding in a minimal cell-free system at the picoliter scale. To compare the antigen binding signal evolution to the actual synthesis of VHH, we determined in each drop the average signal intensity at the particle position and established its distribution among 300 individual drops as a function of time. We measured independently the amount of synthesized VHH at each time point using ELISA after breaking the emulsion. We found that the signal from EGFP accumulated at the capture scaffold was indeed correlated with the evolution of the VHH level along the course of its expression (Figure 3C). Interestingly, significant signal concentration could already be observed in less than 30 min. After 175 min of incubation at 37 °C, a concentration of 6.7 nM of synthesized VHH resulted in a fivefold increase of the EGFP signal per drop on average. Note that this assay involved a number of DNA copies per drop  $\lambda = 300$ . Cell-free expression at the same DNA concentration in bulk led to a yield of 4.9 nM of synthesized VHH after the same incubation time, emphasizing that the encapsulation strategy did not hamper and may even favor the in situ protein synthesis. All these results show that squeezing anti-GFP VHH-coding DNA, its target antigen, and a capture scaffold in microfluidic-generated picoliter drops allows one to quickly achieve VHH synthesis and concomitantly assess its functional binding.

## 2.4. High-Throughput Analysis

After characterizing a large ensemble of drops in parallel, we sought after a flow-based, high-frequency sequential analysis of individual drops offering, for instance, the capability to detect rare events in real-time. This method was implemented not only to characterize the performance of the assay but also to devise a method that could be readily compatible with in situ sorting. To this end, we injected the cell-free expression emulsion after 3 h incubation into another microfluidic device integrating side oil channels to separate the drops and a laser-assisted in situ fluorescence measurement (Figure 4A, left). In this system,

the whole width of the channel was laser-illuminated to ensure a uniform profile of each drop flowing through the measurement window, and the fluorescence emission was recorded by a photomultiplier tube (PMT) detector. The detection of the maximum intensity in each drop fluorescence profile, referred to as Max EGFP, was recorded for a large number of flowing drops and analyzed at a typical frequency of 500 Hz, offering the possibility to explore a pool of thousands of drops in a few seconds only (Figure 4A, right). In particular, we analyzed the drop population produced under the conditions of Figure 3 and analyzed the distribution of Max EGFP, with or without VHH-coding DNA ( $\lambda = 300$ , Figure 4B). Without DNA, the distribution was very sharp and at low Max EGFP values, allowing us to define a threshold (dashed line) above which larger values of Max EGFP would indicate the presence of the produced VHH binding its fluorescent antigen (positive drops). Interestingly, with DNA, the signal was shifted to higher values with the majority of drops (92%, 37 590 events) above the binding threshold, demonstrating both successful synthesis of functional VHH, as well as a good sensitivity of the detection method. In this assay, it was important to optimize the EGFP concentration as the performance of the detection resulted from a tradeoff between antigen amount sufficient to ensure binding detection and low enough to avoid a too strong background inside the drop. For this purpose, we determined how EGFP concentration at a fixed  $\lambda = 300$  affected the distributions of Max EGFP values and we selected a concentration of 40 nM for which positive drops displayed a particularly high signal compared to the background (Figure S8, Supporting Information). We then assessed the minimum number of DNA copies per drop that could be used at this EGFP concentration for the assay to remain applicable. We thus performed our analysis on different emulsions produced with varying NanoGFP-coding DNA concentrations (Figures 4C and Figure S9, Supporting Information). We found that positive drops could be detected at concentrations as low as  $\lambda = 12$ , the fraction of positive drops significantly increasing with an increase in  $\lambda$ . This correlates with the amount of VHH produced in drops. For instance, the VHH concentration for  $\lambda = 12$  was measured to be 0.24 nM, which is about 30 times less than with  $\lambda = 300$ . Notably, at such a low concentration, the fraction of NanoGFP ( $K_D^{app} = 0.26 \pm 0.03$  nM) bound to its antigen can be estimated to be 48%, showing that the detection limit is a sign of inherent VHH affinity. To further demonstrate the applicability of this assay, we added a fluorescently-labeled (Alexa Fluor 647) antibody specific to GFP. We performed the same single-drop analysis in both fluorescent channels on over 80 000 consecutive drops and found that 74% of drops were positive in both channels (Figure S10, Supporting Information). We attribute the relative loss of sensitivity compared to direct EGFP detection (89%) to higher background fluorescence and an increase in steric hindrance on the scaffold when an additional large antibody is present. Interestingly, the large number of detected positive drops in multiple channels shows the possibility of multiplexing the assay, as well as a way to detect non-fluorescent antigens. All these results demonstrate the capability of this method to sequentially analyze large numbers of single drops containing only several copies of VHH-coding DNA and determine the VHH functionality against virtually any kind of antigens, inherently fluorescent or not.

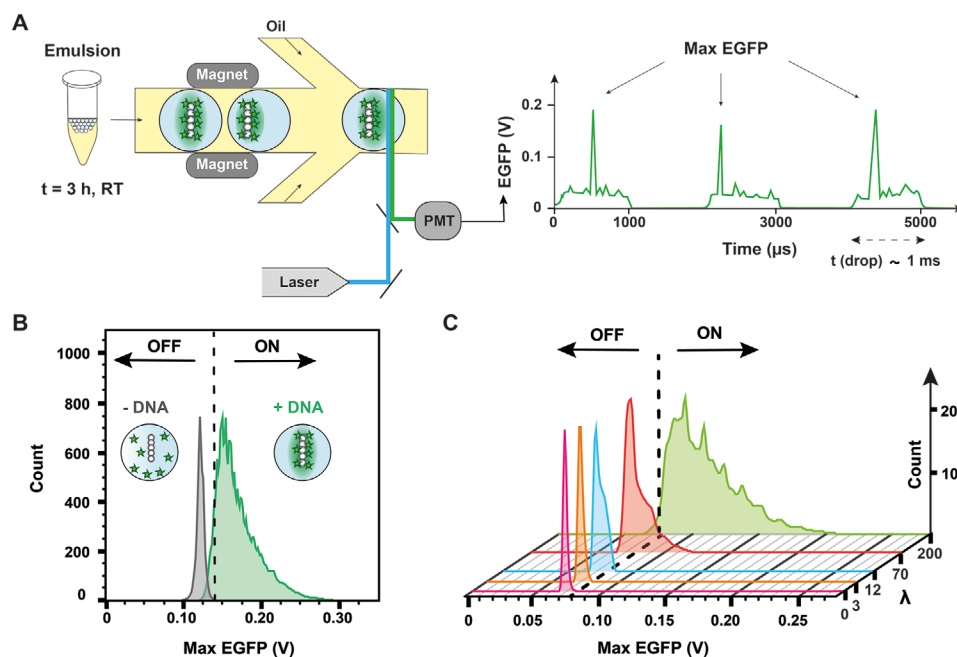


**Figure 4.** Sequential analysis of a large number of droplets reveals VHH-antigen binding can be detected with DNA concentrations as low as  $\lambda = 12$  plasmids per drop. A) Laser and PMT-equipped microfluidic platforms provide a means to differentiate droplets containing target antibodies (binder VHH) from the rest (not expressed or non-binder VHH). After 3 h at 37 °C, the emulsion is injected at RT into a droplet analysis device with magnets used to align the capture scaffolds. Drops are spaced with fluorinated oil with 0.5% of fluorosurfactant and individually flowed in the measurement channel ( $f = 500$  Hz). Upon excitation (488 nm laser), emitted photons (525/40 nm) are converted by a PMT into an electrical signal EGFP (V) and displayed as a function of time (right scheme). For each drop, we detect the maximum signal, referred to as Max EGFP. B) Max EGFP distributions of negative control (–DNA,  $\lambda = 0$ ) and emulsion with DNA coding for NanoGFP (+DNA,  $\lambda = 300$ ). Highest Max EGFP detected for –DNA was fixed as the threshold (dashed line) above which droplets were considered as positive (ON). The distributions represent the signal from 6334 (–DNA) and 37 590 (+DNA) drops. C) Max EGFP distributions for  $\lambda = 0, 3, 12, 70$ , and 200. All emulsions contained EGFP (40 nm). The distributions represent the signal from 782 ( $\lambda = 0$ ), 1021 ( $\lambda = 3$ ), 1681 ( $\lambda = 12$ ), 3003 ( $\lambda = 70$ ), and 8113 ( $\lambda = 200$ ) drops. The total numbers of analyzed droplets (Table S1, Supporting Information) with fractions of positivity per condition (Figure S9, Supporting Information) are available in Supporting Information.

## 2.5. Binding Selectivity

All previous experiments involved a single type of antigen–antibody interaction. To investigate the specificity of cell-free synthesized VHH, we performed the sequential analysis method in the presence of several antigens. As a proof of concept, we encapsulated simultaneously EGFP and the red fluorescent protein mCherry in the drops and we measured both green (EGFP) and red (mCherry) fluorescent signals in the presence of different VHH-coding DNA (Figure 5). With DNA coding for NanoGFP ( $\lambda = 300$ ), the majority of drops (85%) were positive in the green channel while all the drops showed negative signals in the red channel, meaning selective NanoGFP-EGFP binding (Figure 5, top). Conversely, when DNA coding for an anti-mCherry VHH (LaM-4)<sup>[59]</sup> was present ( $\lambda = 500$ ), positive drops were detected with a red channel only (94%, Figure 5, middle), evidencing the selective capture of mCherry by LaM-4. In the case of LaM-4,  $\lambda = 300$  led to a lower proportion of positive drops for the red signal (Figure S11, Supporting Information), which can be attributed to the lower yield of expression of LaM-4 ( $2.8 \pm 0.6 \mu\text{g mL}^{-1}$  in bulk, Figure S3, Supporting Information), comparing to that of NanoGFP ( $15.3 \pm 2 \mu\text{g mL}^{-1}$ ). Without DNA (Figure 5, bottom) no positive signal was detected in either of the channels confirming that the positive peaks in the presence of DNA evidenced selective antigen binding.

## 3. Conclusion

We have demonstrated the possibility to perform an immunoassay using a VHH-coding DNA as a starting material instead of a purified antibody as it is conventionally done. By removing all cell handling and purification steps, functional VHH was synthesized by cell-free expression, and its capability to bind its specific antigen was directly characterized in situ. The whole process took a maximum of 3 h, with binding detectable in less than 30 min, and required minimal amounts of materials and reagents. The assay was performed inside water-in-oil picoliter drops encapsulating the coding DNA, a cell-free expression medium with purified components from *E. coli* (PURExpress, PUREfrex), the target antigen, and magnetic nanoparticles accumulating on their surface the synthesized VHH binding its antigen. Simply incubating such microcompartments at 37 °C under a magnetic field allowed us to follow the accumulation of the antigen signal on the self-assembled nanoparticles, and therefore, assess for the first time the functionality of a cell-free expressed VHH binding its antigen. The HA-tag was conveniently used as a generic and easy-to-implement way to link the synthesized VHH to the particles but other conjugation methods could be envisioned. Similarly, we chose magnetic nanoparticles for their large surface area of binding and capability to self-assemble under command once encapsulated



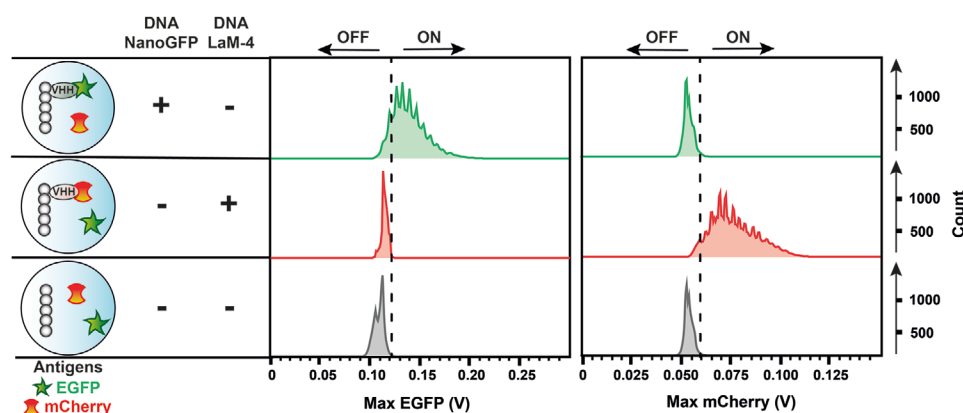


**Figure 5.** Cell-free expressed NanoGFP and LaM-4 present selective antigen binding in the presence of both their target antigens (EGFP and mCherry, respectively). Emulsions with DNA coding for NanoGFP (top row), DNA coding for LaM-4 (middle row), and without DNA (bottom row), all containing both EGFP (40 nm) and mCherry (80 nm), were incubated for 3 h at 37 °C and analyzed using 488 and 561 nm lasers. The detection thresholds (dashed lines) for both channels were determined by the highest Max EGFP and Max mCherry detected in emulsion without DNA. The distributions represent the signal from 31086 (top row, left), 9104 (top row, right), 7771 (middle row, left), 39 978 (middle row, right), 9802 (bottom row, left), and 8005 (bottom row, right) drops. The total numbers of analyzed droplets are available in Supporting Information (Table S1, Supporting Information).

to avoid Poisson partitioning, but other capture scaffolds could be used as well. The concept of the immunoassay was demonstrated here mainly using a DNA coding for an anti-GFP VHH and the corresponding EGFP antigen. Using DNA instead of a preliminarily purified antibody confers to the method a unique degree of programmability that was demonstrated with the successful cell-free synthesis and characterization of different mutants against the same antigen, as well as VHH targeting other antigens (mCherry). By simply adapting the DNA sequence, the method thus offers not only the possibility to virtually implement any VHH but also to modify them in a highly tunable manner (e.g., tag addition, artificial amino acid incorporation, protein truncation/fusion). In our work, all the drops contain the same genetic content but the robustness of cell-free expression in a reconstituted medium makes it readily applicable to library generation and binding assessment. We also showed that the antigen detection was operational with antigens that can be inherently fluorescent (here, EGFP, mCherry) or not (secondary antibody labeling). To avoid possible steric hindrance due to the presence of several secondary IgGs, smaller antibody formats (e.g., F(ab')<sub>2</sub>, F(ab')<sub>1</sub>, or VHH) could be implemented. For a fully DNA-encoded approach, we are also currently implementing the in situ cell-free expression of the antigen itself (data not shown). The panel of antibody–antigen interactions that can be explored with this method thus appears to be potentially extremely large. The microfluidic format of the assay (drop generating device) only requires standard device fabrication and set-ups, thus being implementable in a broad variety of environments, while offering the possibility to work with minimal amounts of reagents at a high speed. We have shown in particular that the picoliter drops containing the DNA-encoded immunoassay could be analyzed individually, in a parallel or sequential manner, at a high frequency (500 Hz) and with amounts of DNA as low as 12 copies per drop. In a synthetic biology context, this work reveals a new facet of cell-free expression that now enables the study of antibody–antigen interaction in a drastically simplified yet highly programmable format. From a biotechnological point of view, this study describes a methodological paradigm shift in immu-

noassay where genetically active synthetic microcompartments produce and directly report the binding activity of their encoded antibody, thus constituting a promising tool for faster discovery and improved implementation of antibodies.

## Supporting Information

Supporting Information is available from the Wiley Online Library or from the author.

## Acknowledgements

The authors thank Nathalie Couteault (Sanofi) and Frédéric Lacroix (Sanofi) for providing access to equipment and experimental support; Vasily Shenshin (Sanofi) for assistance in microfluidic handling; Micaela Vitor (Sanofi), Hélène Erasimus (Sanofi), and Samy Dehissi (Sorbonne Université) for helpful scientific discussions. This work was supported by the National Association of Research Technology ANRT (CIFRE contract 2020/1044), the French National Research Agency ANR (DYOR, contract ANR-18-CE06-0019), and “Institut Pierre-Gilles de Gennes” (laboratoire d'excellence) and “Investissements d'avenir” program ANR-10-IDEX-0001-02 PSL, ANR-10-LABX-31 and ANR-10-EQPX-34.

## Conflict of Interest

The authors declare no conflict of interest.

## Data Availability Statement

The data that support the findings of this study are available from the corresponding author upon reasonable request.

## Keywords

antibody discovery, microfluidics, nanobody, PURE system, synthetic biology

Received: September 23, 2022  
Revised: December 21, 2022  
Published online: February 7, 2023

- [1] I. Sela-Culang, V. Kunik, Y. Ofran, *Front. Immunol.* **2013**, 4, 302.
- [2] I. A. Darwish, *Int. J. Biomed. Sci.* **2006**, 2, 217.
- [3] J. McCafferty, A. D. Griffiths, G. Winter, D. J. Chiswell, *Nature* **1990**, 348, 552.
- [4] R. W. Roberts, J. W. Szostak, *Proc. Natl. Acad. Sci. USA* **1997**, 94, 12297.
- [5] E. T. Boder, K. D. Wittrup, *Nat. Biotechnol.* **1997**, 15, 553.
- [6] J. Hanes, C. Schaffitzel, A. Knappik, A. Plückthun, *Nat. Biotechnol.* **2000**, 18, 1287.
- [7] A. H. Laustsen, V. Greiff, A. Karatt-Vellatt, S. Muyldermans, T. P. Jenkins, *Trends Biotechnol.* **2021**, 39, 1263.
- [8] A. D. Silverman, A. S. Karim, M. C. Jewett, *Nat. Rev. Genet.* **2020**, 21, 151.
- [9] E. D. Carlson, R. Gan, C. E. Hodgman, M. C. Jewett, *Biotechnol. Adv.* **2012**, 30, 1185.
- [10] A. S. M. Salehi, M. T. Smith, A. M. Bennett, J. B. Williams, W. G. Pitt, B. C. Bundy, *Biotechnol. J.* **2016**, 11, 274.
- [11] S. H. Hong, I. Ntai, A. D. Haimovich, N. L. Kelleher, F. J. Isaacs, M. C. Jewett, *ACS Synth. Biol.* **2014**, 3, 398.
- [12] A. Estévez-Torres, C. Crozatier, A. Diguët, T. Hara, H. Saito, K. Yoshikawa, D. Baigl, *Proc. Natl. Acad. Sci. USA* **2009**, 106, 12219.
- [13] D. Kim, T. Kigawa, C. Choi, S. Yokoyama, *Eur. J. Biochem.* **1996**, 239, 881.
- [14] D. Kim, J. R. Swartz, *Biotechnol. Bioeng.* **2004**, 85, 122.
- [15] A. Venancio-Marques, Y. J. Liu, A. Diguët, T. D. Maio, A. Gautier, D. Baigl, *ACS Synth. Biol.* **2012**, 1, 526.
- [16] V. Noireaux, A. Libchaber, *Proc. Natl. Acad. Sci. USA* **2004**, 101, 17669.
- [17] R. Kalmbach, I. Chizhov, M. C. Schumacher, T. Friedrich, E. Bamberg, M. Engelhard, *J. Mol. Biol.* **2007**, 371, 639.
- [18] M. Kaneda, S. M. Nomura, S. Ichinose, S. Kondo, K. Nakahama, K. Akiyoshi, I. Morita, *Biomaterials* **2009**, 30, 3971.
- [19] Y. J. Liu, G. P. R. Hansen, A. Venancio-Marques, D. Baigl, *ChemBioChem* **2013**, 14, 2243.
- [20] J. B. Huppa, H. L. Ploegh, *J. Exp. Med.* **1997**, 186, 393.
- [21] H. Asahara, S. Chong, *Nucleic Acids Res.* **2010**, 38, e141.
- [22] D. Matthies, S. Haberstock, F. Joos, V. Dötsch, J. Vonck, F. Bernhard, T. Meier, *J. Mol. Biol.* **2011**, 413, 593.
- [23] J. Shin, P. Jardine, V. Noireaux, *ACS Synth. Biol.* **2012**, 1, 408.
- [24] P. van Nies, I. Westerlaken, D. Blanken, M. Salas, M. Mencía, C. Danelon, *Nat. Commun.* **2018**, 9, 1583.
- [25] G. Yin, E. D. Garces, J. Yang, J. Zhang, C. Tran, A. R. Steiner, C. Roos, S. Bajad, S. Hudak, K. Penta, J. Zawada, S. Pollitt, C. J. Murray, *mAbs* **2012**, 4, 217.
- [26] M. Stech, S. Kubick, *Antibodies* **2015**, 4, 12.
- [27] S. Murakami, R. Matsumoto, T. Kanamori, *Sci. Rep.* **2019**, 9, 671.
- [28] C. Hamers-Casterman, T. Atarhouch, S. Muyldermans, G. Robinson, C. Hammers, E. B. Songa, R. Hammers, N. Bendahman, *Nat. Methods* **1993**, 363, 446.
- [29] U. Rothbauer, K. Zolghadr, S. Tillib, D. Nowak, L. Schermelleh, A. Gahl, N. Backmann, K. Conrath, S. Muyldermans, M. C. Cardoso, H. Leonhardt, *Nat. Methods* **2006**, 3, 887.
- [30] U. Rothbauer, K. Zolghadr, S. Muyldermans, A. Schepers, M. C. Cardoso, H. Leonhardt, *Mol. Cell Proteomics* **2008**, 7, 282.
- [31] M. Scully, S. R. Cataland, F. Peyvandi, P. Coppo, P. Knöbl, J. A. K. Hovinga, A. Metjian, J. de la Rubia, K. Pavenski, F. Callewaert, D. Biswas, H. D. Winter, R. K. Zeldin, H. Investigators, *N. Engl. J. Med.* **2019**, 380, 335.
- [32] S. Sun, Z. Ding, X. Yang, X. Zhao, M. Zhao, L. Gao, Q. Chen, S. Xie, A. Liu, S. Yin, Z. Xu, X. Lu, *Int. J. Nanomed.* **2021**, 16, 2337.
- [33] S. Vyawahare, A. D. Griffiths, C. A. Merten, *Chem. Biol.* **2010**, 17, 1052.
- [34] R. S. Sista, A. E. Eckhardt, V. Srinivasan, M. G. Pollack, S. Palanki, V. K. Pamula, *Lab Chip* **2008**, 8, 2188.
- [35] M. Y. H. Tang, H. C. Shum, *Lab Chip* **2016**, 16, 4359.
- [36] R. Gao, Z. Cheng, A. J. deMello, J. Choo, *Lab Chip* **2016**, 16, 1022.
- [37] B. Kintsas, L. D. van Vliet, S. R. A. Devenish, F. Hollfelder, *Curr. Opin. Chem. Biol.* **2010**, 14, 548.
- [38] T. M. Tran, F. Lan, C. S. Thompson, A. R. Abate, *J. Phys. D: Appl. Phys.* **2013**, 46, 114004.
- [39] Y. Ding, P. D. Howes, A. J. deMello, *Anal. Chem.* **2020**, 92, 132.
- [40] L. Mazutis, J. Gilbert, W. L. Ung, D. A. Weitz, A. D. Griffiths, J. A. Heyman, *Nat. Protoc.* **2013**, 8, 870.
- [41] K. Eyer, R. C. L. Doineau, C. E. Castrillon, L. Briseño-Roa, V. Menrath, G. Mottet, P. England, A. Godina, E. Brient-Litzler, C. Nizak, A. Jensen, A. D. Griffiths, J. Bibette, P. Bruhns, J. Baudry, *Nat. Biotechnol.* **2017**, 35, 977.
- [42] A. Gérard, A. Woolfe, G. Mottet, M. Reichen, C. Castrillon, V. Menrath, S. Ellouze, A. Poitou, R. Doineau, L. Brisen-Roa, P. Canales-Herrerias, P. Mary, G. Rose, C. Ortega, M. Delincé, S. Essono, B. Jia, B. Iannascoli, O. R.-L. Goff, R. Kumar, S. N. Stewart, Y. Pousse, B. Shen, K. Grosselin, B. Saudemont, A. Sautel-Caillé, A. Godina, S. McNamara, K. Eyer, G. A. Millot, et al., *Nat. Biotechnol.* **2020**, 38, 715.
- [43] P. S. Dittich, M. Jahnz, P. Schwill, *ChemBioChem* **2005**, 6, 811.
- [44] M. Hase, A. Yamada, T. Hamada, D. Baigl, K. Yoshikawa, *Langmuir* **2007**, 23, 348.
- [45] F. Courtois, L. F. Olguin, G. Whyte, D. Bratton, W. T. S. Huck, C. Abell, F. Hollfelder, *ChemBioChem* **2008**, 9, 439.
- [46] A. Sepp, D. S. Tawfik, A. D. Griffiths, *FEBS Lett.* **2002**, 532, 455.
- [47] A. D. Griffiths, D. S. Tawfik, *EMBO J.* **2003**, 22, 24.
- [48] H. M. Cohen, D. S. Tawfik, A. D. Griffiths, *Protein Eng., Des. Sel.* **2004**, 17, 3.
- [49] A. Fallah-Araghi, J. C. Baret, M. Ryckelynck, A. D. Griffiths, *Lab Chip* **2012**, 12, 882.
- [50] Y. Hori, C. Kantak, R. M. Murray, A. R. Abate, *Lab Chip* **2017**, 17, 3037.
- [51] Y. Nagumo, K. Fujiwara, K. Horisawa, H. Yanagawa, N. Doi, *J. Biochem.* **2016**, 159, 519.
- [52] X. Chen, M. Gentili, N. Hacohen, A. Regev, *Nat. Commun.* **2021**, 12, 5506.
- [53] I. Zimmermann, P. Egloff, C. A. Hutter, F. M. Arnold, P. Stohler, N. Bocquet, M. N. Hug, S. Huber, M. Siegrist, L. Hetemmann, J. Gera, S. Gmür, P. Spies, D. Gyax, E. R. Geertsma, R. J. Dawson, M. A. Seeger, *eLife* **2018**, 7, e34317.
- [54] M. H. Kubala, O. Kovtun, K. Alexandrov, B. M. Collins, *Protein Sci.* **2010**, 19, 2389.
- [55] Y. Shimizu, A. Inoue, Y. Tomari, T. Suzuki, T. Yokogawa, K. Nishikawa, T. Ueda, *Nat. Biotechnol.* **2001**, 19, 751.
- [56] S. Muyldermans, *FEBS J.* **2021**, 288, 2084.
- [57] D. Saerens, M. Pellis, R. Loris, E. Pardon, M. Dumoulin, A. Matagne, L. Wyns, S. Muyldermans, K. Conrath, *J. Mol. Biol.* **2005**, 352, 597.
- [58] C. J. Dejournette, J. Kim, H. Medlen, X. Li, L. J. Vincent, C. J. Easley, *Anal. Chem.* **2013**, 85, 10556.
- [59] P. C. Fridy, Y. Li, S. Keegan, M. K. Thompson, I. Nudelman, J. F. Scheid, M. Oeffinger, M. C. Nussenzweig, D. Fenyö, B. T. Chait, M. P. Rout, *Nat. Methods* **2014**, 11, 1253.